Elementary statistical models for collision-sequence interference effects

John Courtenay Lewis*
Department of Physics and Physical Oceanography, Memorial University of Newfoundland, St. John's, Newfoundland, Canada A1B 3X7
(Received 3 March 2008; published 10 June 2008)

In this paper a class of model suitable for application to collision-sequence interference is studied. In these models it is assumed that the intervals between collisions are constant rather than exponentially distributed, as would be true if the collision times formed a Poisson process. The model may be two dimensional or three dimensional. Velocities are assumed to be completely randomized in each collision. The distribution of velocities is assumed to be Gaussian, though use is not always made of that fact. As applied to vector collisional interference the models allow the evaluation of the effects of windowing, which is of importance for $\mathcal{N}$-body simulation of more physically accurate models. They also lead to estimation of the effects of infilling of the interference dip following from deviations of the induced dipole moment from the intermolecular force. As applied to scalar collisional interference the models show the existence of a hitherto unknown (albeit weak) correlation between immediately successive collisions. An extension to the models, in which the magnitude of the induced dipole moment is equal to an arbitrary power or sum of powers of the intermolecular force, allows estimates of the infilling of the interference dip by the disproportionality of the induced dipole moment and force. One particular such model leads to the most realistic estimate for the infilling yet obtained.

DOI: 10.1103/PhysRevA.77.062702 PACS number(s): 34.10.+x, 33.20.Ea, 33.70.−w

I. INTRODUCTION

Spectra resulting from dipole moments induced in molecular collisions typically have the form of broad bands with widths determined by the durations of those collisions [1]. However, these broad bands often exhibit narrow features, which result from the coherence or correlation of induced dipole moments extending over several or many successive collisions. The most conspicuous such features are the vector intercollisional interference dips found in the fundamental bands of H_2-X spectra and in the pure translational bands of mixtures of rare gas atoms [2]. Also well known are scalar collisional interference features found in the R and P transitions in the fundamental bands of HD-X spectra [3–5] and the corresponding R transitions in the pure rotational spectra [6,7]. The term "vector intercollisional interference" refers to the fact that an internal H_2 scalar transition operator is modulated by a vector function of intermolecular displacement. Thus only a Q branch is observed, with the intercollisional dynamics being those which describe the vector property (intermolecular force, to a good approximation) of the external coordinates. The "scalar interference" contribution to the R and P transitions is actually a combination, based upon two effects: an interference between the scalar-modulated internal dipole induced in collisions and the small permanent dipole allowed through a breakdown of the Born-Oppenheimer approximation in the mass-asymmetric HD molecule; and an interference between successive scalar-modulated collisionally induced internal dipole transition moments. The designation "scalar collisional interference" refers to the scalar nature of functions of intermolecular separation (which resemble the intermolecular energy function) that modulate the internal dipole. The collision dynamics of importance are those that influence these functions as the HD molecule experiences them throughout collision sequences. The internal dipole then contributes to $\Delta J = \pm 1$ transitions, and can interfere with any other scalarly modulated internal transition operator having dipole symmetry, including the permanent dipole itself.

Finally, a related, though weaker phenomenon was predicted [8] and observed [9] in collision-induced light scattering. It arises through coherence extending over several collisions in the polarization anisotropy transition amplitudes. This represents a vector-modulated internal second rank tensor transition. In the past it has been labeled "tensor intercollisional interference" which is by more modern terminology somewhat of a misnomer. For simplicity, however, we will continue to use its historic name. Curiously, tensor intercollisional interference leads to interference maxima, as opposed to the dips associated with the vector intercollisional Q branch absorption.

These collision sequence interference effects are thoroughly discussed, and their forms at low densities are found, in Ref. [10]. In this paper we study a class of elementary stochastic models for the scalar and vector interference effects. While these models are simple, the first allows the study of numerical methods such as windowing; and the second allows the demonstration of a correlation effect which has hitherto escaped notice.

II. A CLASS OF MODEL FOR VECTOR INTERFERENCE

At sufficiently low densities and for the study of interference phenomena collisions can be assumed to be instantaneous; the dipole moment induced in one atom or molecule by interaction with a bath of dissimilar atoms or molecules can be represented as

*court@physics.mun.ca

$$\boldsymbol{\mu}(t) = \sum_k \boldsymbol{\mu}_k \delta(t - t_k), \tag{1}$$

where binary collision k occurs at time t_k and the dipole moment induced in collision k is $\boldsymbol{\mu}_k$. For the interference dips in Q branches the quantity $\boldsymbol{\mu}_j$ is parallel to and approximately proportional in magnitude to the impulse (integrated force) $\boldsymbol{f}_k$ experienced by a molecule in the collision. Our models will be expressed in terms of these impulses $\boldsymbol{f}_k$. In general the times t_k approximate to a Poisson process; however, in the present models the particle collisions are supposed to occur at equispaced times. These equispaced collision times can be scaled to be integers, i.e., to lie in $\mathbb{Z}^+$. We will usually index the collisions with k and k'. Then, with appropriate scaling of time, the induced dipole moment as a function of time can be expressed as

$$\boldsymbol{\mu}(t) = \sum_{k \in \mathbb{Z}^+} \boldsymbol{\mu}_k \delta(t - k) \tag{2}$$

instead of Eq. (1). For purposes of analysis we will mainly consider finite random walks with collision times $t_k = k = 0, 1, \ldots, N-1$, and N will usually be taken to be a power of 2.

The positions of the particle at the successive collisions k, $k+1$ are $\boldsymbol{x}_k$ and $\boldsymbol{x}_{k+1}$. The velocities before collisions k and $k+1$ are $\boldsymbol{v}_k$ and $\boldsymbol{v}_{k+1}$, respectively. The impulse suffered by the particle in collision k is given by $\boldsymbol{f}_k = \boldsymbol{v}_{k+1} - \boldsymbol{v}_k$; the particle mass is scaled to be 1. The integrated induced dipole moment $\boldsymbol{\mu}_k$ is approximately proportional to the impulse $\boldsymbol{f}_k$, and for the purposes of the model we will assume initially that the two are equal. This assumption is relaxed in Sec. V.

In the two-dimensional version of the model $\boldsymbol{x}_k$ and $\boldsymbol{v}_k$ and $\boldsymbol{f}_k$ are real two-dimensional vectors. The velocity $\boldsymbol{v}_k = (v_k, \vartheta_k)$ in polar coordinates, and the polar angle ϑ_k is assumed to be uniformly distributed in $[0, 2\pi]$. It is assumed that the velocity before a collision and that after a collision are uncorrelated: $\boldsymbol{v}_k$ and $\boldsymbol{v}_{k+1}$ are assumed to be statistically independent. The persistence of velocity as used in the kinetic theory of gases [11] and the slightly different form used in the study of intercollisional interference [2,12] then is zero. This is a good approximation for a light molecule colliding with a massive one, and a reasonable approximation for collisions between molecules of equal mass, though it fails for mixtures such as H_2-Ar if the Ar velocities are followed.

In consequence of the assumptions made above we have

$$\langle \boldsymbol{v}_i \cdot \boldsymbol{v}_j \rangle = \langle v^2 \rangle \delta_{ij}. \tag{3}$$

In the three-dimensional version of the model the velocity $\boldsymbol{v}_k = (v_k, \vartheta_k, \varphi_k)$, and the polar angles $\Omega_k \equiv (\vartheta_k, \varphi_k)$ are assumed to be uniformly distributed over the unit sphere. Once again Eq. (3) is obtained.

The impulse train

$$\boldsymbol{f}_k = \boldsymbol{v}_{k+1} - \boldsymbol{v}_k \tag{4}$$

has the discrete Fourier transform

$$\boldsymbol{a}_\omega = \sum_{k=0}^{N-1} W^{\omega k} \boldsymbol{f}_k \quad \text{with} \quad \omega = 0, 1, \ldots, N-1 \quad \text{and} \quad W = e^{2\pi\iota/N}. \tag{5}$$

Then the unaveraged periodogram is

$$S_\omega^N = \frac{1}{N} \boldsymbol{a}_\omega \cdot \boldsymbol{a}_\omega^* = \frac{1}{N} \sum_{k,k'} W^{\omega k - \omega k'} \boldsymbol{f}_k \cdot \boldsymbol{f}_{k'}. \tag{6}$$

It is well known that S_ω^N does not converge in probability as $N \to \infty$.

We define the power spectrum of the model intermolecular force to be

$$S_\omega \equiv \frac{1}{N} \langle |\boldsymbol{a}_\omega|^2 \rangle. \tag{7}$$

Now by Eq. (3)

$$\langle \boldsymbol{f}_k \cdot \boldsymbol{f}_{k+2} \rangle = \langle (\boldsymbol{v}_{k+1} - \boldsymbol{v}_k) \cdot (\boldsymbol{v}_{k+3} - \boldsymbol{v}_{k+2}) \rangle = 0, \tag{8a}$$

$$\begin{aligned} \langle \boldsymbol{f}_k \cdot \boldsymbol{f}_{k+1} \rangle &= \langle (\boldsymbol{v}_{k+1} - \boldsymbol{v}_k) \cdot (\boldsymbol{v}_{k+2} - \boldsymbol{v}_{k+1}) \rangle \\ &= -\langle \boldsymbol{v}_{k+1} \cdot \boldsymbol{v}_{k+1} \rangle = -\langle v^2 \rangle, \end{aligned} \tag{8b}$$

$$\langle \boldsymbol{f}_k \cdot \boldsymbol{f}_k \rangle = \langle (\boldsymbol{v}_{k+1} - \boldsymbol{v}_k) \cdot (\boldsymbol{v}_{k+1} - \boldsymbol{v}_k) \rangle = 2\langle v^2 \rangle. \tag{8c}$$

Using these relationships in Eq. (7) we obtain

$$\begin{aligned} S_\omega = \frac{1}{N} \langle |\boldsymbol{a}_\omega|^2 \rangle = \frac{1}{N} \Bigg\{ &\sum_{k=0}^{N-1} \langle \boldsymbol{f}_k \cdot \boldsymbol{f}_k \rangle + \sum_{k=0}^{N-2} W^{-\omega} \langle \boldsymbol{f}_k \cdot \boldsymbol{f}_{k+1} \rangle \\ &+ \sum_{k=1}^{N-1} W^{\omega} \langle \boldsymbol{f}_k \cdot \boldsymbol{f}_{k-1} \rangle \Bigg\}, \end{aligned} \tag{9a}$$

$$= \langle \boldsymbol{f}_k \cdot \boldsymbol{f}_k \rangle \left(1 + 2 \frac{(N-1)}{N} \frac{\langle \boldsymbol{f}_k \cdot \boldsymbol{f}_{k+1} \rangle}{\langle \boldsymbol{f}_k \cdot \boldsymbol{f}_k \rangle} \cos \frac{2\pi\omega}{N} \right), \tag{9b}$$

$$= 2\langle v^2 \rangle \left\{ 1 - \frac{N-1}{N} \cos \frac{2\pi\omega}{N} \right\}, \quad \omega \in [0, N-1]. \tag{9c}$$

The interference dip about $\omega = 0$ does not go precisely to zero for finite N, but rather to

$$\min S = S_0 = \frac{2}{N} \langle v^2 \rangle \tag{10}$$

while the maximum is given by

$$\max S = S_{N/2} = 4 \left(1 - \frac{1}{2N} \right) \langle v^2 \rangle. \tag{11}$$

The ratio is

$$\frac{\min S}{\max S} = \frac{S_0}{S_{N/2}} = \frac{1}{2N - 1}. \tag{12}$$

This same behavior with increasing N is shown in somewhat more complex form in computer simulations [13,14] of the vector interference effect using realistic induced dipole moments and intermolecular forces.

If the autocorrelation function of the induced dipole moment (and force) is defined as the discrete Fourier transform (DFT) of the power spectrum, that is,

$$C_l \equiv \frac{1}{N}\sum_{\omega} W^{\omega l} S_\omega \tag{13}$$

then it follows from Eq. (6) that

$$C_l = \frac{1}{N^2}\sum_{k,k'}\sum_{\omega} W^{\omega(l+k-k')}\langle \boldsymbol{f}_k \cdot \boldsymbol{f}_{k'}\rangle. \tag{14}$$

A modified Kronecker delta function Δ_{ij} can be defined by the conditions

$$\Delta_{ij} = \begin{cases} 1 & \text{if } i = j \bmod N, \\ 0 & \text{otherwise}. \end{cases} \tag{15}$$

Using this definition we find that

$$\sum_{\omega=0}^{N-1} W^{\omega(i-j)} = \Delta_{ij}$$

whence Eq. (14) yields

$$C_l = \frac{1}{N}\sum_{k,k'} \Delta_{l,k'-k}\langle \boldsymbol{f}_k \cdot \boldsymbol{f}_{k'}\rangle = \frac{1}{N}\sum_{k} \langle \boldsymbol{f}_k \cdot \boldsymbol{f}_{k+l \bmod N}\rangle$$

or

$$C_l = \langle \boldsymbol{f}_0 \cdot \boldsymbol{f}_l\rangle, \quad l = 0,1,\ldots,N-1 \tag{16}$$

as the process is stationary. It can readily be shown from Eq. (13) that

$$S_k = \sum_{l=0}^{N-1} W^{-kl} C_l. \tag{17}$$

A. Diffusive motion in the model

The diffusion equation for the probability density $P(\boldsymbol{x})$ governing the position of a particle is given by

$$\frac{\partial P(\boldsymbol{x})}{\partial t} = D\nabla^2 P(\boldsymbol{x})$$

from which it follows that

$$\langle [\boldsymbol{x}(t) - \boldsymbol{x}(0)]^2\rangle = 2dDt,$$

where d is the dimensionality of the model. Hence

$$\langle \boldsymbol{x}_k^2\rangle = \left\langle \left(\sum_{l=0}^{k-1} \boldsymbol{v}_l\right)^2 \right\rangle = k\langle \boldsymbol{v}_l^2\rangle$$

so that the diffusion coefficient is given by

$$D = \frac{\langle \boldsymbol{v}^2\rangle}{2d}.$$

B. Effects of windowing on time series of finite length

One of the useful aspects of our model is that it allows the analytic evaluation of the effects of windowing [18] the data. One of the simplest windows is that of Hann, in which the time series $\boldsymbol{f}_k$ is multiplied by the window function $w_k = 1 - \cos(2\pi k/N)$. A factor of 1/2 is usually included in w_k but we suppress it for computational convenience. We write

$$\tilde{\boldsymbol{a}}_\omega = \sum_{k=0}^{N-1} W^{\omega k} w_k \boldsymbol{f}_k. \tag{18}$$

The normalization coefficient for the windowed power spectrum is

$$\tilde{w}_{ss} = \sum_{k=0}^{N-1} w_k^2 = \frac{3}{2}N.$$

The windowed but unaveraged periodogram is given by

$$\tilde{S}_\omega^N = \frac{1}{W_{ss}} \tilde{\boldsymbol{a}}_\omega \cdot \tilde{\boldsymbol{a}}_\omega^*. \tag{19}$$

Substitution of Eq. (18) into Eq. (19) yields, after averaging,

$$\langle |\tilde{\boldsymbol{a}}_\omega|^2\rangle = \sum_{k=0}^{N-1} \langle \boldsymbol{f}_k \cdot \boldsymbol{f}_k\rangle w_k^2 + \sum_{k=0}^{N-2} W^{-\omega}\langle \boldsymbol{f}_k \cdot \boldsymbol{f}_{k+1}\rangle w_k w_{k+1} + \sum_{k=1}^{N-1} W^{\omega}\langle \boldsymbol{f}_k \cdot \boldsymbol{f}_{k-1}\rangle w_k w_{k-1} \tag{20a}$$

$$= 2\langle v^2\rangle \left\{ \sum_{k=0}^{N-1} w_k^2 - \cos\frac{2\pi\omega}{N} \sum_{k=0}^{N-2} w_k w_{k+1} \right\}. \tag{20b}$$

It can be shown that

$$w_k w_{k+1} = \sum_{k=0}^{N-2} \left(1 - \cos\frac{2\pi k}{N}\right)\left(1 - \cos\frac{2\pi(k+1)}{N}\right) = \frac{3N}{2} - \frac{N}{2}\left(1 - \cos\frac{2\pi}{N}\right).$$

Hence the "Hanned" spectrum becomes

$$\tilde{S}_\omega = \frac{2}{3N} 2\langle v^2\rangle \left\{ \frac{3N}{2} - \cos\frac{2\pi\omega}{N}\left[\frac{3N}{2} - \frac{N}{2}\left(1 - \cos\frac{2\pi}{N}\right)\right]\right\} = 2\langle v^2\rangle \left\{ 1 - \cos\frac{2\pi\omega}{N}\left[1 - \frac{1}{3}\left(1 - \cos\frac{2\pi}{N}\right)\right]\right\}. \tag{21}$$

The minimum of the windowed spectrum thus is given by

$$\tilde{S}_0 = \frac{2}{3}\langle v^2\rangle\left(1 - \cos\frac{2\pi}{N}\right) = \langle v^2\rangle\left(\frac{4\pi^2}{3N^2} + O(N^{-4})\right) \tag{22}$$

which can be compared with Eq. (10), which gives the minimum without windowing. The spectral maximum is given by

$$\max \tilde{S} = \tilde{S}_{N/2} = 4\langle v^2\rangle\left\{1 - \frac{1}{6}\left(1 - \cos\frac{2\pi}{N}\right)\right\} = 4\langle v^2\rangle\left\{1 - \frac{\pi^2}{3N^2} + O(N^{-4})\right\} \tag{23}$$

which can be compared with Eq. (11). Finally,

$$\frac{\min \tilde{S}}{\max \tilde{S}} = \frac{\tilde{S}_0}{\tilde{S}_{N/2}} = \frac{\pi^2}{3N^2} + O(N^{-4}) \tag{24}$$

which can be compared with Eq. (12). It is evident from these comparisons that "Hanning" the data improves the estimation of the minimum, the maximum, and the ratio of minimum to maximum by a factor of order N^{-1}. In typical molecular dynamics studies of vector intercollisional interference [13,14] N is of the order of 10^5 or greater so "Hanning" the data very significantly improves the accuracy of a spectrum obtained by molecular dynamics in the vicinity of an interference dip.

III. SCALAR INTERFERENCE

For the pure scalar interference effect, with the contributions from the allowed weak dipole neglected, we have

$$\mu(t) = \sum_{k \in \mathbb{Z}} \mu_k \delta(t-k) \tag{25}$$

with, as a first approximation,

$$\mu_k = f_k = |\boldsymbol{f}_k|. \tag{26}$$

The relevant induced dipole moment is discussed in detail in Ref. [3]. The Fourier transform of $\mu(t)$ is given by

$$a_\omega = \sum_{k=0}^{N-1} W^{\omega k} f_k. \tag{27}$$

Then the averaged periodogram is given by

$$S_\omega^N = \frac{1}{N} \langle |a_\omega|^2 \rangle. \tag{28}$$

We have

$$\langle |a_\omega|^2 \rangle = \sum_{k=0}^{N-1} \sum_{k'=0}^{N-1} W^{\omega(k-k')} \langle f_k f_{k'} \rangle. \tag{29}$$

Now $f_k = |\boldsymbol{f}_k| = |\boldsymbol{v}_{k+1} - \boldsymbol{v}_k|$ so that $\langle f_k f_{k'} \rangle = \langle f_k \rangle^2$ unless $k = k'$ or $k = k' \pm 1$. Hence,

$$\langle |a_\omega|^2 \rangle = \langle f \rangle^2 \sum_{k=0}^{N-1} \sum_{k'=0}^{N-1} W^{\omega(k-k')} + \sum_{k=0}^{N-1} (\langle f^2 \rangle - \langle f \rangle^2) + \sum_{k=0}^{N-2} W^{-\omega} (\langle f_k f_{k+1} \rangle - \langle f \rangle^2) + \sum_{k=1}^{N-1} W^{\omega} (\langle f_k f_{k-1} \rangle - \langle f \rangle^2), \tag{30a}$$

$$= N^2 \langle f \rangle^2 \delta_{\omega,0} + N \operatorname{var} f + (N-1) e^{-2\pi \iota \omega / N} \operatorname{cov}(f_k, f_{k+1}) + (N-1) e^{2\pi \iota \omega / N} \operatorname{cov}(f_k, f_{k-1}), \tag{30b}$$

or

$$S_\omega^N = N \langle f \rangle^2 \delta_{\omega,0} + \operatorname{var} f + 2\left(1 - \frac{1}{N}\right) \cos \frac{2\pi\omega}{N} \operatorname{cov}(f_k, f_{k+1}). \tag{31}$$

The first term gives the positive collisional interference peak. The second term gives the constant background. If the actual duration of the induced dipole moment pulses were included, this term would give the broad peak characteristic of collision-induced spectra. The third term is the most interesting, as it expresses the effect of the correlation in force between successive collisions. The existence of this correlation had not been suspected prior to this present work.

A. Evaluation of $\langle f^2 \rangle$ and $\langle f_k f_{k+1} \rangle$ in three dimensions

In three dimensions $f_k^n \equiv |\boldsymbol{v}_{k+1} - \boldsymbol{v}_k|^n$ can be expanded in spherical harmonics [15,16] as

$$f_k^n \equiv |\boldsymbol{v}_{k+1} - \boldsymbol{v}_k|^n = 4\pi \sum_{l=0}^{\infty} \sum_{m=-l}^{l} \frac{1}{2l+1} a_l^n(v_{k+1}, v_k) Y_{lm}(\Omega_{k+1}) Y_{lm}^*(\Omega_k), \tag{32}$$

where expressions for the coefficients a_l^n are given in pp. 166–167 of Ref. [16]. One such expression for a_l^n is

$$a_l^n(r_1, r_2) = \frac{\left(-\frac{n}{2}\right)_l}{\left(\frac{1}{2}\right)_l} r_2^n \left(\frac{r_1}{r_2}\right)^l {}_2F_1\left(l - \frac{n}{2}, -\frac{1}{2} - \frac{n}{2}; l + \frac{3}{2}; \frac{r_1^2}{r_2^2}\right), \quad r_1 < r_2. \tag{33}$$

Averaging Eq. (32) over Ω_k and Ω_{k+1} yields

$$\langle f^n \rangle = \langle a_0^n(v_{k+1}, v_k) \rangle. \tag{34}$$

Hence

$$\langle f \rangle^2 = \langle a_0^1(v_{k+1}, v_k) \rangle^2 \tag{35}$$

and

$$\operatorname{var} f = \langle a_0^2(v_{k+1}, v_k) \rangle - \langle a_0^1(v_{k+1}, v_k) \rangle^2. \tag{36}$$

Assuming that the velocities obey Gaussian distributions with unit variance, i.e.,

$$P(\boldsymbol{v}) = \frac{1}{(2\pi)^{3/2}} e^{-(1/2)v^2},$$

then using numerical integration it is found that

$$\langle a_0^2(v_{k+1}, v_k) \rangle = 6, \tag{37a}$$

$$\langle a_0^1(v_{k+1}, v_k) \rangle = 2.256758, \tag{37b}$$

and

$$\operatorname{var} f = 0.90704. \tag{38}$$

For the cross term we have

$$f_k f_{k+1} = (4\pi)^2 \sum_{l,m} \sum_{l',m'} \left(\frac{1}{2l+1}\right) \times \left(\frac{1}{2l'+1}\right) a_{l'}^1(v_{k+2},v_{k+1}) a_l^1(v_{k+1},v_k) \times Y_{l'm'}(\Omega_{k+2}) Y_{l'm'}^*(\Omega_{k+1}) Y_{lm}(\Omega_{k+1}) Y_{lm}^*(\Omega_k) \tag{39}$$

from which it follows that

$$\langle f_k f_{k+1}\rangle = (4\pi)^2 \frac{1}{(4\pi)^2} (\sqrt{4\pi})^2 \langle a_0^1(v_{k+2},v_{k+1}) a_0^1(v_{k+1},v_k) \times Y_{00}^*(\Omega_{k+1}) Y_{00}(\Omega_{k+1})\rangle = \langle a_0^1(v_{k+2},v_{k+1}) a_0^1(v_{k+1},v_k)\rangle \tag{40}$$

whence

$$\mathrm{cov}(f_k,f_{k+1}) = \langle a_0^1(v_{k+2},v_{k+1}) a_0^1(v_{k+1},v_k)\rangle - \langle a_0^1(v_{k+1},v_k)\rangle^2. \tag{41}$$

Integrating the above numerically yields

$$\langle a_0^1(v_{k+2},v_{k+1}) a_0^1(v_{k+1},v_k)\rangle = 5.307973 \tag{42}$$

which gives, finally,

$$\mathrm{cov}(f_k,f_{k+1}) = 0.21502. \tag{43}$$

The moments of f require the evaluation of two–dimensional integrals of not particularly simple form, as can be seen from Eq. (34), while evaluation of $\langle f_k f_{k+1}\rangle$ requires a three-dimensional integral, over the speeds v_{k+2}, v_{k+1}, v_k.

The nonvanishing covariance of f_k and f_{k+1} comes from the fact that f_k and f_{k+1} share the common velocity $\mathbf{v}_{k+1}$, or more accurately the common speed v_{k+1}. If v_{k+1} is well above its mean value then on average both $f_k = |\boldsymbol{v}_{k+1} - \boldsymbol{v}_k|$ and $f_{k+1} = |\boldsymbol{v}_{k+2} - \boldsymbol{v}_{k+1}|$ will be larger than their means, and similarly if v_{k+1} is smaller than its mean value then f_k and f_{k+1} will tend to be small. The nonvanishing of $\mathrm{cov}(f_k,f_{k+1})$ is an effect of varying particle speed: for a constant-speed velocity distribution $\mathrm{cov}(f_k,f_{k+1})=0$. To see this we note that if $v_k = v = \mathrm{const}\ \ \forall k$ then Eq. (41) reduces to

$$\mathrm{cov}(f_k,f_{k+1}) = \langle a_0^1(v_{k+2},v_{k+1}) a_0^1(v_{k+1},v_k)\rangle - \langle a_0^1(v_{k+1},v_k)\rangle^2 = a_0^1(v,v) a_0^1(v,v) - a_0^1(v,v)^2 = 0. \tag{44}$$

Thus collision processes which randomize direction but not speed will give a nonzero correlation between f_k and f_{k+1}. The correlation should be smaller for collisions between, say, HD and Ar or Xe, which will randomize the direction of the HD but not its speed, than for HD-He collisions, which partially randomize both direction and speed.

It is noteworthy that the form of the scalar spectrum depends on the distribution of velocities though the form of the vector spectrum does not. The variance in the vector spectrum does, however, depend on the distribution of velocities.

B. Evaluation of $\langle f^2\rangle$ and $\langle f_k f_{k+1}\rangle$ in two dimensions

To evaluate terms of the form $\langle f_k f_{k'}\rangle$, we set $0=\varphi_k = \varphi_{k+1} = \varphi_{k'} = \varphi_{k'+1}$ in Eq. (32) and use the addition theorem for spherical harmonics to obtain

$$f_k^n f_{k'}^{n'} \equiv |\boldsymbol{v}_{k+1} - \boldsymbol{v}_k|^n |\boldsymbol{v}_{k'+1} - \boldsymbol{v}_{k'}|^{n'} = \sum_{l=0}^{\infty} \sum_{l'=0}^{\infty} a_l^n(v_{k+1},v_k) a_{l'}^{n'}(v_{k'+1},v_{k'}) \times \mathrm{P}_l(\cos(\vartheta_{k+1} - \vartheta_k)) \mathrm{P}_{l'}(\cos(\vartheta_{k'+1} - \vartheta_{k'})). \tag{45}$$

This yields

$$\langle f_k^n f_{k'}^{n'}\rangle = \sum_{l=0}^{\infty} \langle a_l^n(v_{k+1},v_k) a_{l'}^{n'}(v_{k'+1},v_{k'})\rangle \times \langle \mathrm{P}_l(\cos(\vartheta_{k+1} - \vartheta_k)) \mathrm{P}_{l'}(\cos(\vartheta_{k'+1} - \vartheta_{k'}))\rangle. \tag{46}$$

Because, in two dimensions,

$$\langle \mathrm{P}_l(\cos(x))\rangle = \frac{1}{2\pi} \int_0^{2\pi} \mathrm{P}_l(\cos x) dx \neq 0 \quad \text{for even } l$$

and more generally $\langle \mathrm{P}_l(\cos(\vartheta_{k+1} - \vartheta_k)) \mathrm{P}_{l'}(\cos(\vartheta_{k'+1} - \vartheta_{k'}))\rangle \neq 0$ for an infinite number of l,l' the series (46) in two dimensions will not terminate. A more tractable approach to the evaluation of $\langle f_k^n f_{k'}^{n'}\rangle$, specific to Gaussian velocity distributions, is set forth in the following section. It is easily seen from the expression $\langle f_k f_{k+1}\rangle = \langle |\boldsymbol{v}_{k+1} - \boldsymbol{v}_k| |\boldsymbol{v}_{k+2} - \boldsymbol{v}_{k+1}|\rangle$ that, for a constant-speed distribution, $\langle f_k f_{k+1}\rangle = \langle f_k\rangle\langle f_{k+1}\rangle$ and hence $\mathrm{cov}\, f_k f_{k+1} = 0$ as we had previously found to be the case in three dimensions.

C. Evaluation of $\langle f^2\rangle$ and $\langle f_k f_{k+1}\rangle$ for Gaussian distribution of velocities in two dimensions

If the distribution of velocities is taken to be Gaussian with unit variance, then in two dimensions the probability density for $\mathbf{v}$ is given by

$$P(\boldsymbol{v}) = \frac{1}{2\pi} e^{-(1/2)v^2}.$$

Hence

$$\langle f^n\rangle = \frac{1}{4\pi^2} \int d^2v d^2v' e^{-(1/2)(v^2+v'^2)} |\boldsymbol{v} - \boldsymbol{v}'|^n.$$

This expression can be evaluated using the variables $\boldsymbol{u} = \boldsymbol{v} - \boldsymbol{v}'$ and $\boldsymbol{U} = \frac{1}{2}(\boldsymbol{v} + \boldsymbol{v}')$. Clearly $v^2 + v'^2 = \frac{1}{2}u^2 + 2U^2$. The Jacobian of the transformation is unity. Hence

$$\langle f^n\rangle = \frac{1}{4\pi^2}\int d^2u d^2U\, e^{-(1/4)u^2-U^2}u^n$$
$$= \left(\int_0^\infty dU\, Ue^{-U^2}\right)\left(\int_0^\infty du e^{-(1/4)u^2}u^{n+1}\right)$$
$$= 2^n\int_0^\infty dw\, e^{-w}w^{n/2} = 2^n\Gamma\left(\frac{n}{2}+1\right). \quad (47)$$

In particular

$$\langle f\rangle = 2\Gamma\left(\frac{3}{2}\right) = \Gamma\left(\frac{1}{2}\right) = \sqrt{\pi} \quad \text{and} \quad \langle f^2\rangle = 4. \quad (48)$$

Then

$$\text{var}\, f = 4 - \pi = 0.85841. \quad (49)$$

For the cross term we have

$$\langle f_k f_{k+1}\rangle = \frac{1}{8\pi^3}\int d^2v d^2v' d^2v'' e^{-1/2(v^2+v'^2+v''^2)}|\boldsymbol{v}-\boldsymbol{v}'||\boldsymbol{v}'-\mathbf{v}''|. \quad (50)$$

We set $\boldsymbol{u}=\boldsymbol{v}-\boldsymbol{v}'$ and $\boldsymbol{u}'=\boldsymbol{v}'-\boldsymbol{v}''$ and $\boldsymbol{U}=\frac{1}{2}(\boldsymbol{v}+\boldsymbol{v}'+\boldsymbol{v}'')$ so that

$$\begin{pmatrix}\boldsymbol{v}\\ \boldsymbol{v}'\\ \boldsymbol{v}''\end{pmatrix} = \begin{pmatrix}\frac{2}{3}\boldsymbol{u}+\frac{1}{3}\boldsymbol{u}'+\frac{2}{3}\boldsymbol{U}\\ -\frac{1}{3}\boldsymbol{u}+\frac{1}{3}\boldsymbol{u}'+\frac{2}{3}\boldsymbol{U}\\ -\frac{1}{3}\boldsymbol{u}-\frac{2}{3}\boldsymbol{u}'+\frac{2}{3}\boldsymbol{U}\end{pmatrix} \quad (51)$$

and

$$\frac{1}{2}(v^2+v'^2+v''^2) = \frac{1}{3}u^2+\frac{1}{3}\boldsymbol{u}\cdot\boldsymbol{u}'+\frac{1}{3}u'^2+\frac{2}{3}U^2. \quad (52)$$

The Jacobian of the transformation is

$$\begin{vmatrix}\frac{2}{3} & \frac{1}{3} & \frac{2}{3}\\ -\frac{1}{3} & \frac{1}{3} & \frac{2}{3}\\ -\frac{1}{3} & -\frac{2}{3} & \frac{2}{3}\end{vmatrix} = \frac{2}{3}.$$

Then

$$\langle f_k f_{k+1}\rangle$$
$$= \frac{1}{18\pi^3}\int d^2u d^2u' d^2U e^{-[(1/3)u^2+(1/3)\boldsymbol{u}\cdot\boldsymbol{u}'+(1/3)u'^2+(2/3)U^2]}uu'$$
$$= \frac{9}{2\pi}\int_0^\infty du\int_0^\infty du'\int_0^{2\pi} d\vartheta u^2u'^2$$
$$\times\exp\{-(u^2+uu'\cos\vartheta+u'^2)\}, \quad (53)$$

where $\vartheta = \measuredangle\,\boldsymbol{u},\boldsymbol{u}'$. Using the Rayleigh expansion

$$e^{z\cos\vartheta} = I_0(z) + 2\sum_{k=1}^\infty I_k(z)\cos(k\vartheta)$$

in Eq. (53) yields

$$\langle f_k f_{k+1}\rangle = 9\int_0^\infty du\int_0^\infty du' u^2u'^2\exp(-u^2-u'^2)I_0(uu')$$
$$= 3.3412. \quad (54)$$

Hence the covariance of f_k and f_{k+1} is given by

$$\text{cov}(f_k,f_{k+1}) = 3.3412 - \pi = 0.19957. \quad (55)$$

The covariance of f_k and f_{k+1} thus is about one-quarter of the variance in f_k.

The above result can also be recovered analytically. We have

$$\langle f_k f_{k+1}\rangle = 9\int_0^\infty du\int_0^\infty du' u^2u'^2\exp(-u^2-u'^2)I_0(uu')$$
$$= 9\sum_{k=0}^\infty \frac{\left(\frac{1}{2}\right)^{2k}}{\Gamma(k+1)k!}\int_0^\infty du\int_0^\infty du' u^{2+2k}(u')^{2+2k}$$
$$\times\exp(-u^2-u'^2) = \frac{9}{4}\sum_{k=0}^\infty \frac{\left(\frac{1}{2}\right)^{2k}\Gamma\left(k+\frac{3}{2}\right)^2}{\Gamma(k+1)k!}$$
$$= \frac{9\Gamma\left(\frac{3}{2}\right)^2}{4\Gamma(1)}\sum_{k=0}^\infty \frac{\left(\frac{3}{2}\right)_k^2}{(1)_k k!}\left(\frac{1}{4}\right)^k$$

or

$$\langle f_k f_{k+1}\rangle = \frac{9\pi}{16}{}_2F_1\left(\frac{3}{2},\frac{3}{2};1;\frac{1}{4}\right) \quad (56)$$

and this, in turn, gives

$$\langle f_k f_{k+1}\rangle = 3.34122$$

in agreement with Eq. (54) above.

The positivity of the spectrum in Eq. (31) necessitates that

$$\text{var}\, f \geq 2|\text{cov}(f_k,f_{k+1})|. \quad (57)$$

It is apparent from Eqs. (49) and (55) that this inequality is satisfied in two dimensions, and from Eqs. (38) and (43) that it is satisfied in three dimensions.

The two-dimensional spectrum for $N=512$ is shown in Figs. 1 and 2. Figure 1 shows theory and simulation, averaged over 100 repetitions, over the whole spectral range, while Fig. 2 shows the region around the peak only. The dip which is evident around $\omega=256$ is due to a third correlation term $2(1-1/N)\cos(2\pi\omega/N)\text{cov}(f_k,f_{k+1})$ in Eq. (31).

IV. THE ALLOWED COMPONENT

In the absence of shifting and broadening mechanisms the inclusion of the allowed part of the transition in the dipole

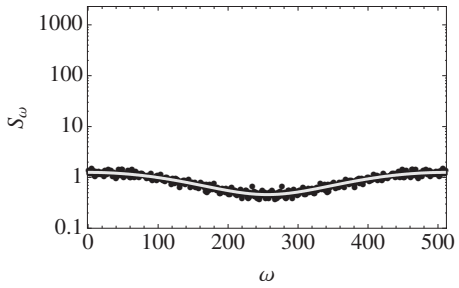

FIG. 1. Two-dimensional spectrum. The simulation results are shown as dots, while the theoretical spectrum as given by Eq. (31) is shown in light gray.

moment can be represented by adding a constant to Eq. (25) giving

$$\mu(t) = A + \sum_{k\in\mathbb{Z}} \mu_k \delta(t-k) \tag{58}$$

with $\mu_k = f_k = |\boldsymbol{f}_k|$ as above. The Fourier transform of $\mu(t)$ is given by

$$a_\omega = NA\,\delta_{\omega 0} + \sum_{k=0}^{N-1} W^{\omega k} f_k. \tag{59}$$

The averaged periodogram is, as above, given by

$$S_\omega^N = \frac{1}{N}\langle |a_\omega|^2 \rangle$$

so that

$$\begin{aligned}\langle |a_\omega|^2 \rangle &= N^2A^2\delta_{\omega 0} + NA\,\delta_{\omega 0}\sum_{k=0}^{N-1}(W^{\omega k} + W^{-\omega k})\langle f_k\rangle \\ &+ \sum_{k=0}^{N-1}\sum_{k'=0}^{N-1} W^{\omega(k-k')}\langle f_k f_{k'}\rangle = N^2A^2\delta_{\omega 0} + 2N^2A\langle f\rangle\delta_{\omega 0} \\ &+ \sum_{k=0}^{N-1}\sum_{k'=0}^{N-1} W^{\omega(k-k')}\langle f_k f_{k'}\rangle. \end{aligned} \tag{60}$$

As above, $\langle f_k f_{k'}\rangle = \langle f_k\rangle^2$ unless $k=k'$ or $k=k'\pm 1$, with the same consequences as above. Hence

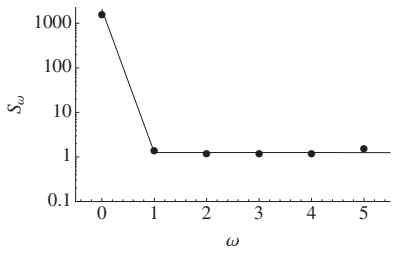

FIG. 2. Two-dimensional spectrum near the origin. The simulation results are shown as dots, while the theoretical spectrum as given by Eq. (31) is shown as a solid line.

$$\begin{aligned}\langle |a_\omega|^2 \rangle &= N^2A^2\delta_{\omega 0} + 2N^2A\langle f\rangle\delta_{\omega 0} + N^2\langle f\rangle^2\delta_{\omega,0} + N\,\mathrm{var}\,f \\ &+ (N-1)e^{-2\pi\iota\omega/N}\,\mathrm{cov}(f_k, f_{k+1}) \\ &+ (N-1)e^{2\pi\iota\omega/N}\,\mathrm{cov}(f_k, f_{k-1})\end{aligned}$$

or

$$\begin{aligned}S_\omega^N &= N(A^2 + 2A\langle f\rangle + \langle f\rangle^2)\delta_{\omega,0} + \mathrm{var}\,f \\ &+ 2\left(1 - \frac{1}{N}\right)\cos\frac{2\pi\omega}{N}\mathrm{cov}(f_k, f_{k+1}).\end{aligned} \tag{61}$$

Only the peak at $\omega=0$ is altered by the addition of the constant term to the train of induced dipole moment pulses. Because both A and μ_k have been assumed to be real, the well-known interference [10] between the allowed and the induced components is not captured by this model.

V. GENERALIZATION OF THE MODEL FOR VECTOR INTERCOLLISIONAL INTERFERENCE

The dipole moment or transition moment induced in a collision is not in fact exactly proportional to the intermolecular force; the overlap parts differ in range by about 25%. The deviation from exact proportionality leads to a partial infilling of the interference dip, and almost from the beginning of theoretical studies in the subject methods have been sought to relate the infilling to the differences between the induced dipole moment and the intermolecular force. In that context it is interesting to generalize the model for vector intercollisional interference by taking the induced dipole moment to be parallel to the intermolecular force, but with magnitude proportional to some nonlinear function of the magnitude of the intermolecular force; specifically, we consider

$$\boldsymbol{\mu}_k = \boldsymbol{f}_k(1 + \alpha f_k^\nu) \equiv \beta(|\boldsymbol{v}_{k+1} - \boldsymbol{v}_k|)(\boldsymbol{v}_{k+1} - \boldsymbol{v}_k), \tag{62a}$$

$$\beta(v) = 1 + \alpha v^\nu, \tag{62b}$$

where ν is some positive constant, and α is a constant which physically is small with respect to 1. Then the impulse train of induced dipole moments is $\{\boldsymbol{\mu}_k\}_k$ rather than Eq. (4), and its DFT is

$$\boldsymbol{a}_\omega = \sum_{k=0}^{N-1} W^{\omega k}\boldsymbol{\mu}_k \quad \text{with} \quad \omega = 0, 1, \ldots, N-1 \tag{63}$$

instead of Eq. (5). The unaveraged periodogram becomes

$$S_\omega^N = \frac{1}{N}\sum_{k,k'} W^{\omega k - \omega k'}\boldsymbol{\mu}_k\cdot\boldsymbol{\mu}_{k'} \tag{64}$$

instead of Eq. (6).

Now as in Eq. (3) $\boldsymbol{v}_k$ is uncorrelated with $\boldsymbol{v}_k'$ if $|k'-k| > 1$, with the consequence that

$$\begin{aligned}&\langle \boldsymbol{\mu}_k\cdot\boldsymbol{\mu}_{k'}\rangle \\ &= \langle \beta(|\boldsymbol{v}_{k+1} - \boldsymbol{v}_k|)\beta(|\boldsymbol{v}_{k'+1} - \boldsymbol{v}_k'|)(\boldsymbol{v}_{k+1} - \boldsymbol{v}_k)\cdot(\boldsymbol{v}_{k'+1} - \boldsymbol{v}_{k'})\rangle \\ &= 0\end{aligned} \tag{65}$$

for $|k'-k| > 1$. Using Eq. (65) in Eq. (64) we obtain

$$S_\omega = \frac{1}{N}\langle |\boldsymbol{a}_\omega|^2\rangle, \tag{66a}$$

$$= \frac{1}{N}\left\{ \sum_{k=0}^{N-1} \langle \boldsymbol{\mu}_k \cdot \boldsymbol{\mu}_k\rangle + \sum_{k=0}^{N-2} W^{-\omega}\langle \boldsymbol{\mu}_k \cdot \boldsymbol{\mu}_{k+1}\rangle + \sum_{k=1}^{N-1} W^{\omega}\langle \boldsymbol{\mu}_k \cdot \boldsymbol{\mu}_{k-1}\rangle \right\}, \tag{66b}$$

$$= \langle \boldsymbol{\mu}_k \cdot \boldsymbol{\mu}_k\rangle \left(1 + 2\frac{(N-1)}{N}\frac{\langle \boldsymbol{\mu}_k \cdot \boldsymbol{\mu}_{k+1}\rangle}{\langle \boldsymbol{\mu}_k \cdot \boldsymbol{\mu}_k\rangle}\cos\frac{2\pi\omega}{N}\right),$$

$$\omega \in [0, N-1]. \tag{66c}$$

If we take the limit $N \to \infty$ with $\tilde{\omega} \equiv 2\pi\omega/N$ held constant then Eq. (66a)–(66c) yields

$$S_{\tilde{\omega}} = \langle \boldsymbol{\mu}_k \cdot \boldsymbol{\mu}_k\rangle \left(1 + 2\frac{\langle \boldsymbol{\mu}_k \cdot \boldsymbol{\mu}_{k+1}\rangle}{\langle \boldsymbol{\mu}_k \cdot \boldsymbol{\mu}_k\rangle}\cos\tilde{\omega}\right). \tag{67}$$

It is evident, therefore, that the spectrum is determined by the two moments $\langle \boldsymbol{\mu}_k \cdot \boldsymbol{\mu}_k\rangle$ and $\langle \boldsymbol{\mu}_k \cdot \boldsymbol{\mu}_{k+1}\rangle$.

From Eq. (66a)–(66c) the minimum and maximum of the spectrum $S_{\tilde{\omega}}$ are given by

$$\max S_{\tilde{\omega}} = \langle \boldsymbol{\mu}_k \cdot \boldsymbol{\mu}_k\rangle, \tag{68a}$$

$$\min S_{\tilde{\omega}} = \langle \boldsymbol{\mu}_k \cdot \boldsymbol{\mu}_k\rangle + 2\langle \boldsymbol{\mu}_k \cdot \boldsymbol{\mu}_{k+1}\rangle. \tag{68b}$$

The first of these moments is straightforward. We have

$$\langle \boldsymbol{\mu}_k \cdot \boldsymbol{\mu}_k\rangle = \langle \boldsymbol{f}_k \cdot \boldsymbol{f}_k (1 + \alpha f_k^\nu)^2\rangle = \langle f^2\rangle + 2\alpha\langle f^{\nu+2}\rangle + \alpha^2\langle f^{2\nu+2}\rangle. \tag{69}$$

For a two-dimensional Gaussian distribution of velocities we have, from Eq. (47),

$$\langle \boldsymbol{\mu}_k \cdot \boldsymbol{\mu}_k\rangle = 4 + \alpha 2^{\nu+3}\Gamma\left(\frac{\nu}{2}+2\right) + \alpha^2 2^{2\nu+2}\Gamma(\nu+2). \tag{70}$$

For the case $\nu = 1$ this gives

$$\langle \boldsymbol{\mu}_k \cdot \boldsymbol{\mu}_k\rangle = 4 + 21.26945\alpha + 32\alpha^2. \tag{71}$$

The second of the moments is rather more involved. We have

$$\langle \boldsymbol{\mu}_k \cdot \boldsymbol{\mu}_{k+1}\rangle = \langle \boldsymbol{f}_k \cdot \boldsymbol{f}_{k+1}(1 + \alpha f_k^\nu)(1 + \alpha f_{k+1}^\nu)\rangle = \langle (\boldsymbol{v} - \boldsymbol{v}') \cdot (\boldsymbol{v}' - \boldsymbol{v}'')(1 + \alpha|\boldsymbol{v} - \boldsymbol{v}'|^\nu)(1 + \alpha|\boldsymbol{v}' - \boldsymbol{v}''|^\nu)\rangle. \tag{72}$$

We set $\boldsymbol{u} = \boldsymbol{v} - \boldsymbol{v}'$ and $\boldsymbol{u}' = \boldsymbol{v}' - \boldsymbol{v}''$ and $\boldsymbol{U} = \frac{1}{2}(\boldsymbol{v} + \boldsymbol{v}' + \boldsymbol{v}'')$ as in Sec. III B and find that

$$\langle \boldsymbol{\mu}_k \cdot \boldsymbol{\mu}_{k+1}\rangle = \langle (\boldsymbol{u} \cdot \boldsymbol{u}')(1 + \alpha u^\nu)(1 + \alpha u'^\nu)\rangle = \langle uu' \cos\vartheta\rangle + 2\alpha\langle u^{\nu+1}u' \cos\vartheta\rangle + \alpha^2\langle u^{\nu+1}(u')^{\nu+1}\cos\vartheta\rangle \tag{73}$$

with $\vartheta = \measuredangle \boldsymbol{u}, \boldsymbol{u}'$. Introducing the function $\mathcal{J}$ defined by

$$\mathcal{J}(\mu, \nu) \equiv -\langle u^\mu (u')^\nu \cos\vartheta\rangle. \tag{74}$$

Equation (73) reduces to

$$\langle \boldsymbol{\mu}_k \cdot \boldsymbol{\mu}_{k+1}\rangle = -\mathcal{J}(1,1) - 2\alpha\mathcal{J}(\nu+1,1) - \alpha^2\mathcal{J}(\nu+1,\nu+1). \tag{75}$$

Extending the treatment of the integration in Eq. (53) above we obtain

$$\mathcal{J}(\mu,\nu) = -\frac{1}{12\pi^2}\int d^2u d^2u' e^{-(1/3)(u^2 + \boldsymbol{u}\cdot\boldsymbol{u}' + u'^2)} u^\mu (u')^\nu \cos\vartheta$$

$$= -\frac{3^{[(\mu+\nu)/2]+1}}{4\pi^2}\int d^2u d^2u' e^{-(u^2 + \boldsymbol{u}\cdot\boldsymbol{u}' + u'^2)} u^\mu (u')^\nu \cos\vartheta$$

$$= -\frac{3^{[(\mu+\nu)/2]+1}}{2\pi}\int_0^\infty du \int_0^\infty du' \int_0^{2\pi} d\vartheta u^{\mu+1}(u')^{\nu+1} \times \cos\vartheta \exp\{-(u^2 + uu'\cos\vartheta + u'^2)\}. \tag{76}$$

As

$$e^{z\cos\vartheta} = I_0(z) + 2\sum_{k=1}^\infty I_k(z)\cos(k\vartheta)$$

we have

$$\mathcal{J}(\mu,\nu) = 3^{[(\mu+\nu)/2]+1}\int_0^\infty du \int_0^\infty du' u^{\mu+1}(u')^{\nu+1}\exp(-u^2 - u'^2) I_1(uu')$$

$$= 3^{[(\mu+\nu)/2]+1}\sum_{k=0}^\infty \frac{\left(\frac{1}{2}\right)^{2k+1}}{\Gamma(k+2)k!}\int_0^\infty du \int_0^\infty du' u^{\mu+2+2k}(u')^{\nu+2+2k}\exp(-u^2 - u'^2)$$

$$= \frac{3^{[(\mu+\nu)/2]+1}}{8}\sum_{k=0}^\infty \frac{\left(\frac{1}{2}\right)^{2k}\Gamma\left(\frac{\mu}{2}+\frac{3}{2}+k\right)\Gamma\left(\frac{\nu}{2}+\frac{3}{2}+k\right)}{\Gamma(k+2)k!}$$

$$= \frac{3^{[(\mu+\nu)/2]+1}\Gamma\left(\frac{\mu}{2}+\frac{3}{2}\right)\Gamma\left(\frac{\nu}{2}+\frac{3}{2}\right)}{8\Gamma(2)}\sum_{k=0}^\infty \frac{\left(\frac{\mu}{2}+\frac{3}{2}\right)_k\left(\frac{\nu}{2}+\frac{3}{2}\right)_k}{(2)_k k!}\left(\frac{1}{4}\right)^k$$

or

$$\mathcal{J}(\mu,\nu)=\frac{3^{[(\mu+\nu)/2]+1}\Gamma\left(\frac{\mu}{2}+\frac{3}{2}\right)\Gamma\left(\frac{\nu}{2}+\frac{3}{2}\right)}{8}\times{}_2F_1\left(\frac{\mu}{2}+\frac{3}{2},\frac{\nu}{2}+\frac{3}{2};2;\frac{1}{4}\right). \tag{77}$$

Clearly

$$\mathcal{J}(1,1)=2 \tag{78}$$

and for the case $\nu=1$ we obtain

$$\mathcal{J}(2,1)=3\sqrt{\pi}=5.31736 \quad \text{and} \quad \mathcal{J}(2,2)=14.5838. \tag{79}$$

It can be shown that

$$\mathcal{J}(\nu+1,1)=2^{\nu+1}\Gamma\left(\frac{\nu}{2}+2\right) \tag{80}$$

whence

$$\min S_{\tilde{\omega}}=2\alpha^2[2^{2\nu+1}\Gamma(\nu+2)-\mathcal{J}(\nu+1,\nu+1)]. \tag{81}$$

For $\nu=1$ this yields

$$\min S_{\tilde{\omega}}=2\alpha^2(16-14.5838)=2.8324\alpha^2, \tag{82a}$$

$$\frac{\min S_{\tilde{\omega}}}{\max}S_{\tilde{\omega}}=0.7081\alpha^2+O(\alpha^4). \tag{82b}$$

This is in accord with earlier work ([2] and references therein) on the infilling of the interference dip in which the spectral minimum was found to be proportional to an average of $(f_k\mu_{k'}-f_{k'}\mu_k)^2$.

The power-law model. A realistic model for the induced dipole moment in systems such as He-H_2 can be obtained [17] by taking

$$\boldsymbol{\mu}_k=\boldsymbol{f}_k f_k^{\nu} \tag{83}$$

with $\nu\approx-0.25$. Then by Eq. (81) we have

$$\min S_{\tilde{\omega}}=2[2^{2\nu+1}\Gamma(\nu+2)-\mathcal{J}(\nu+1,\nu+1)] \tag{84}$$

with $\mathcal{J}$ given by Eq. (77), while from Eqs. (68a), (68b), (69), and (70) the spectral maximum is given by

$$\max S_{\tilde{\omega}}=2^{2\nu+2}\Gamma(\nu+2). \tag{85}$$

It can be shown that for small ν Eq. (84) yields

$$\min S_{\tilde{\omega}}=O(\nu^2) \tag{86}$$

and

$$\left.\frac{\min S_{\tilde{\omega}}}{\max S_{\tilde{\omega}}}\right|_{\nu=-0.25}=0.0088399. \tag{87}$$

Although the infilling of the interference dip because of dissimilarities (disproportionalities in magnitude) between the intermolecular force and the induced dipole moment has been estimated previously [2], the power model with $\nu=-0.25$ is the most realistic model for which it has been possible to carry through the calculations.

VI. CONCLUSIONS

In this paper we have developed a class of model for the study of collision-sequence interference effects in collision-induced absorption. In these models a single particle is followed. Its collisions are supposed to be instantaneous, and to occur at equally spaced times. Velocities are supposed to be completely randomized at each collision. It is supposed that the dipole moment $\boldsymbol{\mu}_k$ or μ_k induced in a collision is proportional to the integrated intermolecular force $\boldsymbol{f}_k$ or f_k, respectively, or, in Sec. V, a power or sum of powers of the integrated intermolecular force.

An important feature of this class of model is that the model spectra can be determined analytically, or at worst reduced to straightforward numerical integrations. Quantitative estimation of interference for records of finite length have been obtained, which are useful in the context of error estimation for $\mathcal{N}$-body simulations. We find, for example, that for vector interference the ratio of interference minimum to spectral maximum depends on record length N as $O(N^{-1})$. It is also possible to work out exactly the effects of windowing procedures, and we find that the principal effect of the Hann window is to reduce the ratio of interference minimum to spectral maximum to $O(N^{-2})$, which for typical $\mathcal{N}$-body simulations where record length is $O(10^3)$ collisions is most useful.

In the theory of scalar interference, our treatment leads to a previously unexpected correlation among immediately successive induced dipole moment amplitudes. This correlation depends on the randomization of particle speeds rather than directions in collisions.

The extension of the induced dipole moment model to dipole moments which are proportional to an arbitrary power of the integrated intermolecular force shows that the interference dip is partially filled in for any disproportionality between induced dipole moment and integrated induced dipole moment. However, for a realistic value of the power the infilling is slight, being about 1% of spectral maximum.

Most features of the models considered in the present work can be extended to more realistic models in which the collision times are Poisson distributed and, for scalar interference, models in which the dipole moments are complex. Such extensions are necessary to determine whether the correlation found in the scalar interference effect, and characterized by $\langle f_k f_{k+1}\rangle\neq 0$ are of significance in observed spectra in real spectra. These topics will be examined in a subsequent paper.

ACKNOWLEDGMENTS

We thank Roger M. Herman for many useful discussions on collision-sequence interference and other aspects of spectroscopy, and for a number of suggestions in regard to this present work. We thank the Department of Physics of the Pennsylvania State University, and its Head, Dr. Jayanth Banavar, for their hospitality. We acknowledge support from the Natural Sciences and Engineering Research Council of Canada.

[1] L. Frommhold, *Collision-induced Absorption in Gases* (Cambridge University Press, Cambridge, 1993).
[2] J. C. Lewis, in *Phenomena Induced by Intermolecular Interactions*, edited by G. Birnbaum (Plenum Press, New York, 1985), pp. 215–257.
[3] R. M. Herman, Phys. Rev. Lett. **42**, 1206 (1979).
[4] R. M. Herman, R. H. Tipping, and J. D. Poll, Phys. Rev. A **20**, 2006 (1979).
[5] R. M. Herman, in *Spectral Line Shapes Vol. 10*, Proceedings of the 14th International Conference on Spectral Line Shapes, edited by R. M. Herman, AIP Conf. Proc. No. 467 (American Institute of Physics, Woodbury, NY, 1999), pp. 552–555.
[6] J. B. Nelson and G. C. Tabisz, Phys. Rev. A **28**, 2157 (1983).
[7] A. R. W. McKellar, J. W. C. Johns, W. Majewski, and N. H. Rich, Can. J. Phys. **62**, 1673 (1984).
[8] J. C. Lewis and J. van Kranendonk, Can. J. Phys. **50**, 2902 (1972).
[9] L. Ulivi, N. Meinander, and F. Barocchi, Phys. Rev. Lett. **75**, 3094 (1995).
[10] J. C. Lewis and R. M. Herman, Phys. Rev. A **68**, 032703 (2003).
[11] S. Chapman and T. G. Cowling, *The Mathematical Theory of Non-Uniform Gases*, 2nd ed. (Cambridge University Press, Cambridge, 1964).
[12] J. C. Lewis, Can. J. Phys. **50**, 2881 (1972).
[13] R. M. Herman and J. C. Lewis, in *Spectral Line Shapes Vol. 12*, Proceedings of the 16th International Conference on Spectral Line Shapes, edited by C. A. Back, AIP Conf. Proc. No. 645 (American Institute of Physics, Melville, NY, 2002), pp. 233–236.
[14] J. C. Lewis, in *Proceedings of the 17th International Conference on Spectral Line Shapes*, edited by E. Dalimier (Frontier Group, 2004), pp. 369–371.
[15] R. A. Sack, J. Math. Phys. (Cambridge, Mass.) **37**, 215 (1957).
[16] D. A. Varshalovich, A. N. Moskalev, and V. K. Khersonskii, *Quantum Theory of Angular Momentum* (World Scientific, Singapore, 1988).
[17] R. M. Herman and J. C. Lewis, Phys. Rev. B **73**, 155408 (2006).
[18] Herman informs me that windowing in numerical analysis is analogous to the phenomenon of "apodization" in physical optics.